Cancer Cell
Article

Gene-Targeting of *Phd2* Improves Tumor Response to Chemotherapy and Prevents Side-Toxicity

Rodrigo Leite de Oliveira,[1,2,3,4,10] Sofie Deschoemaeker,[1,3,10] Anne-Theres Henze,[1,3] Koen Debackere,[1,3] Veronica Finisguerra,[1,3] Yukiji Takeda,[1,2,3,4] Carmen Roncal,[1,2,3,4,5] Daniela Dettori,[1,2,3,4] Evelyne Tack,[1,3] Yannick Jönsson,[1,3] Lorenzo Veschini,[1,3] Annelies Peeters,[6] Andrey Anisimov,[8] Matthias Hofmann,[9] Kari Alitalo,[8] Myriam Baes,[6] Jan D'hooge,[7] Peter Carmeliet,[2,4] and Massimiliano Mazzone[1,3,*]
[1]Lab of Molecular Oncology and Angiogenesis
[2]Lab of Angiogenesis and Neurovascular Link
Vesalius Research Center, VIB, 3000 Leuven, Belgium
[3]Lab of Molecular Oncology and Angiogenesis
[4]Lab of Angiogenesis and Neurovascular Link, Department of Oncology
Vesalius Research Center, KU Leuven, 3000 Leuven, Belgium
[5]Atherosclerosis Research Laboratory, CIMA-University of Navarra, 31008 Pamplona, Spain
[6]Laboratory of Cell Metabolism
[7]Division of Cardiovascular Imaging and Dynamics
KU Leuven, 3000 Leuven, Belgium
[8]Molecular/Cancer Biology Laboratory, Research Programs Unit, Institute for Molecular Medicine, 00014 Helsinki, Finland
[9]Department of Dermatology, Johann Wolfgang Goethe-University, 60590 Frankfurt am Main, Germany
[10]These authors contributed equally to this work
*Correspondence: massimiliano.mazzone@vib-kuleuven.be
http://dx.doi.org/10.1016/j.ccr.2012.06.028

SUMMARY

The success of chemotherapy in cancer treatment is limited by scarce drug delivery to the tumor and severe side-toxicity. Prolyl hydroxylase domain protein 2 (PHD2) is an oxygen/redox-sensitive enzyme that induces cellular adaptations to stress conditions. Reduced activity of PHD2 in endothelial cells normalizes tumor vessels and enhances perfusion. Here, we show that tumor vessel normalization by genetic inactivation of *Phd2* increases the delivery of chemotherapeutics to the tumor and, hence, their antitumor and antimetastatic effect, regardless of combined inhibition of *Phd2* in cancer cells. In response to chemotherapy-induced oxidative stress, pharmacological inhibition or genetic inactivation of *Phd2* enhances a hypoxia-inducible transcription factor (HIF)-mediated detoxification program in healthy organs, which prevents oxidative damage, organ failure, and tissue demise. Altogether, our study discloses alternative strategies for chemotherapy optimization.

INTRODUCTION

Part of the failure that still escorts cancer treatment is due to the abnormal tumor vasculature, characterized by leaky, tortuous, and fragile vessels; loss of hierarchical architecture; and an abnormal endothelial layer. The resultant hypoxia promotes invasion and metastasis (Carmeliet and Jain, 2011). In addition, hypoperfused vessels and increased interstitial tumor pressure impede the delivery of anticancer drugs to the tumors and thus limit their efficacy (Carmeliet and Jain, 2011).

To date, anti-vascular endothelial growth factor and anti-vascular endothelial growth factor receptor [VEGF(R)] approaches have therefore gained interest as a therapeutic option to improve drug delivery and the overall response to anticancer treatment,

Significance

Chemotherapy remains the most common treatment option for cancer patients. However, dysfunctional blood vessels and severe side effects impede delivery of chemotherapeutic drugs to the tumor, thus limiting their use in the clinic. Traditional antiangiogenic strategies can worsen this situation by hindering tumor perfusion and exacerbating adverse reactions. Here, we identify PHD2 as a molecular target to enhance chemotherapeutic drug delivery to the tumor via vessel normalization and to counter chemotherapy-induced side effects via a HIF-mediated detoxification response. These data unveil an essential role of PHD2 as gatekeeper for oxidative stress, and they warrant caution for considerate use of HIF blockers in cancer in association with chemotherapy. Taken together, our study offers the rationale for developing PHD2 specific inhibitors for cancer therapy.

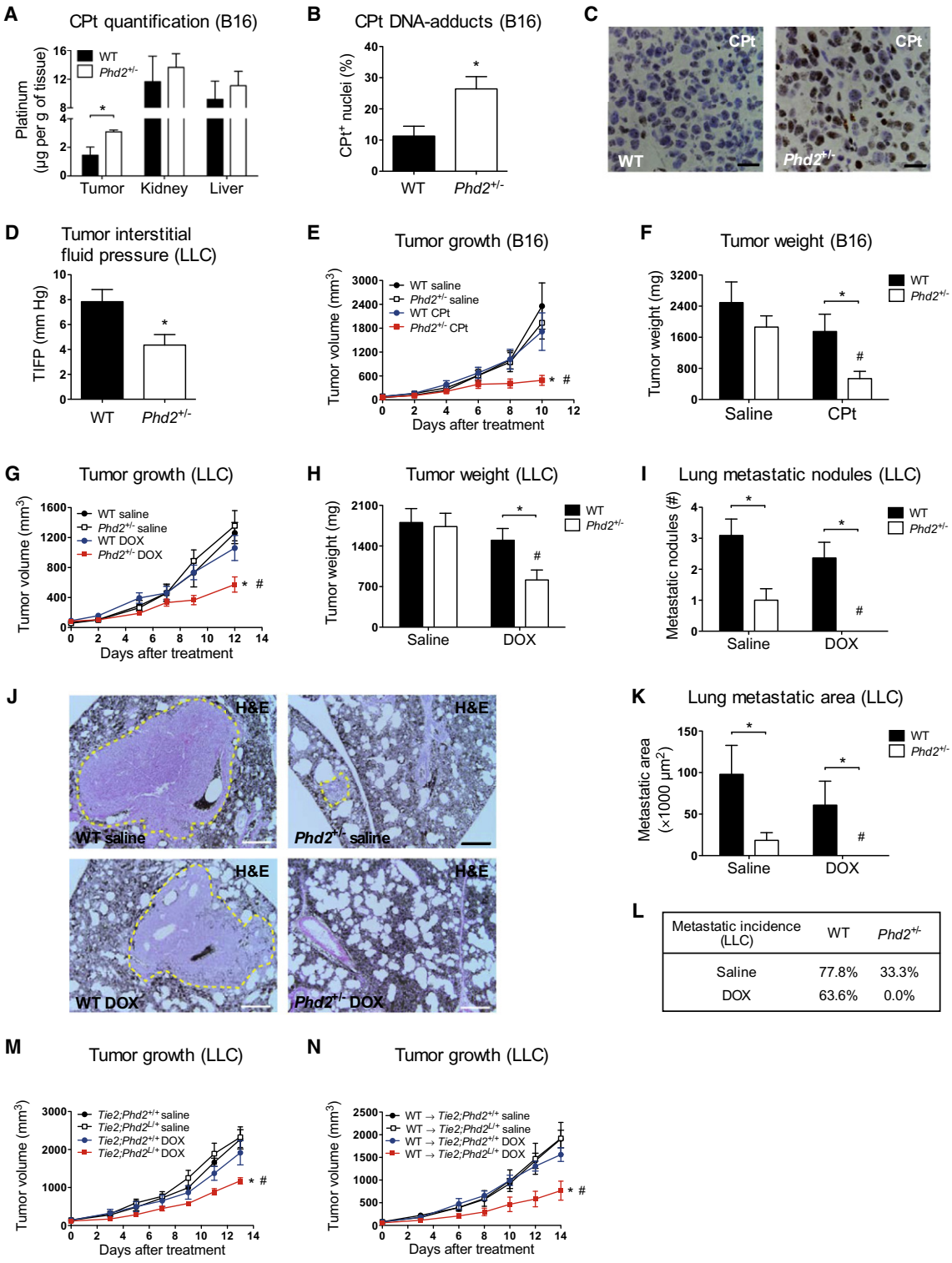

Metastatic incidence (LLC)	WT	*Phd2*$^{+/-}$
Saline	77.8%	33.3%
DOX	63.6%	0.0%

Figure 1. Stromal *Phd2* Haplodeficiency Enhances Tumor Response to Chemotherapy

(A) Platinum levels (as readout of cisplatin, CPt) in tumors and healthy organs (kidney and liver) of WT and *Phd2*$^{+/-}$ mice (n = 4–5).

(B and C) Quantification (B) and representative images (C) showing increased intratumoral CPt DNA-adducts in *Phd2*$^{+/-}$ mice (n = 3).

(D) Interstitial fluid pressure of LLC tumors is decreased in *Phd2*$^{+/-}$ mice (n = 6–7).

(E–H) Reduced growth and weight of B16 melanoma tumors (E and F) or LLC tumors (G and H) in *Phd2*$^{+/-}$ mice upon suboptimal doses (2.5 mg/kg; 3× per week) of CPt or doxorubicin (DOX), respectively (n = 5–9).

(I) Number of lung metastatic nodules in LLC tumor-bearing mice (n = 5–6).

given their ability to promote tumor vessel normalization in preclinical and clinical studies (Carmeliet and Jain, 2011; Goel et al., 2011). Nonetheless, this concept has been recently challenged by the observation that bevacizumab, a humanized monoclonal antibody that blocks VEGF, reduces both perfusion and tumor drug uptake in non-small cell lung cancer patients (Van der Veldt et al., 2012). Importantly, current antiangiogenic therapies are more toxic than anticipated, particularly when used in combination with chemotherapeutic drugs (D'Adamo et al., 2005). Alternative approaches have been evaluated in preclinical tumor models in order to increase the local concentration of chemotherapeutics, either by normalizing tumor blood flow (Fischer et al., 2007; Rolny et al., 2011; Stockmann et al., 2008) or by using tumor specific deliveries (Dhar et al., 2011; Jain, 2010). However, so far, none of the strategies tested show efficient drug delivery to the tumor and simultaneous protection of vital organs, thus optimizing the cytostatic efficiency of the drug and preventing undesired, life-threatening toxic effects.

Prolyl hydroxylase domain proteins (PHD1-3) are enzymes that utilize oxygen to hydroxylate and target the alpha subunit of the hypoxia-inducible transcription factors HIF-1 and HIF-2 for proteasomal degradation (Epstein et al., 2001). When oxygen tension drops, PHDs become less active, leading to hypoxia-inducible transcription factor (HIF) stabilization and, consequently, to the initiation of an adaptive response, including angiogenesis, metabolic reprogramming, erythropoiesis, and scavenging of reactive oxygen species (ROS) (Aragonés et al., 2008; Lee et al., 1997; Mukhopadhyay et al., 2000; Scortegagna et al., 2003). By using cancer as a model of abnormal angiogenesis, we recently showed that heterozygous deficiency of *Phd2* (also known as *Egln1*) in endothelial cells (EC) does not affect vessel density or lumen size, but normalizes their endothelial lining, barrier, stability, and pericyte coverage, at least in part, via HIF-2-mediated upregulation of the adherens junction vascular endothelial-cadherin and the soluble VEGF trap sFlt1. This change in vessel structure and endothelial shape improves tumor perfusion and oxygenation and, hence, inhibits cancer cell intravasation and metastasis (Mazzone et al., 2009). Moreover, gene deletion or knockdown of *Phd1* confers tissue protection against ischemia/reperfusion-induced oxidative damage (Aragonés et al., 2008; Schneider et al., 2010); conversely, reduced activity of HIF-1 or HIF-2 has been associated to increased ROS production and, thereby, tissue dysfunction in both normal and stress conditions (Lee et al., 1997; Mukhopadhyay et al., 2000; Scortegagna et al., 2003). This has critical implications in cancer therapy, since both chemotherapeutic- and irradiation-based treatments generate ROS that impair normal organ function and cause tissue demise (Anscher et al., 2005; Berthiaume and Wallace, 2007; Pabla and Dong, 2008).

In the present study, we investigate the biological and therapeutic relevance of gene-targeting the oxygen/redox-sensitive enzyme PHD2 in different cell compartments on the tumor response to chemotherapy. At the same time, we pursue a mechanistic understanding on how pharmacological and genetic inhibition of PHD2 affects chemotherapy-associated ROS production in healthy organs and, subsequently, tissue damage and function.

RESULTS

Stromal Loss of *Phd2* Sensitizes the Tumor to Chemotherapy

We recently showed that endothelial haplodeficiency of *Phd2* ($Phd2^{+/-}$) streamlines the tumor vasculature (Mazzone et al., 2009). Prompted by these results, we examined whether partial loss of *Phd2* also enhances the delivery of chemotherapeutic drugs. We therefore subjected wild-type (WT) and $Phd2^{+/-}$ mice carrying equal-size B16 melanomas to a single dose of cisplatin (20 mg/kg) and measured platinum accumulation in tumor, kidney, and liver 1 hr after drug injection. While normal organs showed similar cisplatin concentrations in both WT and $Phd2^{+/-}$ mice (Figure 1A), intratumoral platinum and drug diffusion out of the tumor vessels was higher in $Phd2^{+/-}$ than in WT mice (Figures 1A–1C), the latter being consistent with a reduction of tumor interstitial fluid pressure (Figure 1D), a physical parameter hindering efficient transit of drugs within the tumor (Heldin et al., 2004).

To assess whether the improved drug delivery translated into enhanced antitumor effects, we treated B16 tumor-bearing mice with a suboptimal dose of cisplatin (2.5 mg/kg; 3× per week), which did not have any therapeutic effect in WT mice (Figures 1E and 1F). In contrast, end-stage tumor volume and tumor weight were reduced in $Phd2^{+/-}$ mice by more than 70% (Figures 1E and 1F). We then extended our study to a different tumor histotype, i.e., Lewis lung adenocarcinoma (LLC), which was treated with doxorubicin. A suboptimal dose of doxorubicin (2.5 mg/kg; 3× per week) did not affect the growth of subcutaneously implanted LLC tumors in WT mice, whereas it reduced end-stage volume and weight by about 60% in $Phd2^{+/-}$ mice (Figures 1G and 1H). As previously shown (Mazzone et al., 2009), number, area, and incidence of pulmonary metastasis were reduced in $Phd2^{+/-}$ versus WT untreated mice (Figures 1I–1L). Doxorubicin treatment did not affect metastatic burden in WT mice, while it completely prevented metastasis formation in $Phd2^{+/-}$ mice, likely due to the strong inhibition of primary tumor growth (Figures 1G–1L). Deletion of one *Phd2* allele in EC, but not in myeloid cells or in fibroblasts, induced chemosensitization of LLC tumors to a suboptimal dose of doxorubicin (Figures 1M and 1N; Figures S1A and S1B available online).

In B16 tumors, suboptimal doses of cisplatin promoted tumor cell apoptosis and reduced proliferation in $Phd2^{+/-}$ mice (Figures

(J and K) Representative micrographs (J) and morphometric quantification (K) of hematoxylin and eosin (H&E)-stained lung sections revealing reduced metastatic area (yellow dashed line) in $Phd2^{+/-}$ LLC tumor-bearing mice and no metastases in $Phd2^{+/-}$ mice treated with DOX (n = 5–6).

(L) Metastatic incidence in LLC tumor-bearing mice (n = 5–6).

(M and N) LLC tumor growth in response to suboptimal doses of DOX (2.5 mg/kg; 3× per week) in $Tie2;Phd2^{L/+}$ mice (M; n = 6–9) or in $Tie2;Phd2^{L/+}$ and $Tie2;Phd2^{+/+}$ mice transplanted with WT bone marrow, WT → $Tie2;Phd2^{L/+}$ and WT → $Tie2;Phd2^{+/+}$, respectively (N; n = 5–9). The bone marrow transplantation is to ensure that *Phd2* is not deleted in the hematopoietic compartment, where the $Tie2^{Cre}$ deleter is also active.

*$p < 0.05$ versus WT, #$p < 0.05$ versus saline. Scale bars denote 20 μm in (C) and 200 μm in (J). All graphs show mean ± SEM. See also Figure S1.

2A–2F and Table S1). In doxorubicin-treated LLC tumors, apoptosis, but not proliferation, was higher in $Phd2^{+/-}$ versus WT mice (Figures 2G and 2H and Table S1). Tumor apoptosis and proliferation did not change in WT and $Phd2^{+/-}$ untreated mice (Figures 2B, 2C, and 2E–2H and Table S1).

Cytostatic drugs can display some antiangiogenic effects (Kerbel and Kamen, 2004). However, baseline and posttreatment tumor vessel perfusion and oxygenation were comparably higher in $Phd2^{+/-}$ versus WT mice, despite similar vessel density and area (Figures 2I–2N). Similarly, endothelial *Phd2* haplodeficiency increased tumor perfusion in both doxorubicin-treated and untreated mice (Figure S2).

Altogether, these data show that reduction of *Phd2* in EC enhances the response of the tumor to chemotherapy by increasing vessel perfusion and drug delivery.

Acute Loss of One or Two *Phd2* Alleles Enhances Chemotherapy

The above findings show that constitutive deletion of *Phd2* in EC induces tumor vessel normalization and thus increases tumor response to chemotherapeutics. To assess the effect of inducible deletion of *Phd2* on chemoresponse, we intercrossed *Phd2*-floxed mice with the tamoxifen-inducible $Rosa26^{CreERT2}$ mouse strain, where the *Rosa26* (*R26*) promoter directs the ubiquitous expression of the fusion protein Cre-ERT2. We also exploited this system to compare the effect of heterozygous ($R26;Phd2^{L/+}$) versus homozygous ($R26;Phd2^{L/L}$) deletion, leading, respectively, to about 50% and 2%–5% of the PHD2 protein levels in different tissues of WT ($R26;Phd2^{+/+}$) mice (Figures 3A and S3A and Table S2). In vitro, primary EC isolated from $R26;Phd2^{L/+}$ and $R26;Phd2^{L/L}$ mice displayed increasing accumulation of HIF-1α (Figure 3A and Table S2). Conversely, HIF-2α was higher, but elevated to the same level in both $R26;Phd2^{L/+}$ and $R26;Phd2^{L/L}$ primary EC, likely due to compensatory mechanisms promoted by induction of *Phd3* (Figures 3A and S3B and Table S2).

In vivo, deletion of one or two *Phd2* alleles in stromal cells (achieved by tamoxifen administration for 5 consecutive days following LLC cell injection) did not alter tumor growth in untreated mice, but was equally potent in sensitizing the tumor to the effect of doxorubicin (Figures 3B and 3C). Metastatic dissemination was almost completely prevented in both $R26;Phd2^{L/+}$ and $R26;Phd2^{L/L}$ mice after doxorubicin (Figure 3D). Features of tumor vessel normalization, as vessel coverage (Figures 3E and 3F), vessel perfusion (Figures 3G and S3C), and tumor oxygenation (Figure 3H), were promoted in both doxorubicin-treated and untreated $R26;Phd2^{L/+}$ and $R26;Phd2^{L/L}$ mice.

Vegf is an oxygen-sensitive gene that is strongly expressed by the tumor in response to hypoxia as well as oncogenic activation (Semenza, 2003). Previous reports have shown that systemic levels of VEGF following postnatal deletion of *Phd2* increase or can remain unchanged, depending on the experimental settings (Minamishima et al., 2008; Takeda et al., 2007). Thirty days after genetic deletion of *Phd2* (i.e., about the duration of our tumor experiments), plasma levels of VEGF were slightly increased by 12% and 29%, respectively, in $R26;Phd2^{L/+}$ and $R26;Phd2^{L/L}$ tumor-free mice (Figure 3I). In tumor-bearing mice, as expected, VEGF levels were generally higher, but in both $R26;Phd2^{L/+}$ and $R26;Phd2^{L/L}$ tumor-bearing mice, these levels were lower than in $R26;Phd2^{+/+}$ tumor-bearing mice, because vessel normalization and improved oxygenation partly prevented VEGF production by the tumor itself (Figures 3I and 3J).

The effect of *Phd2* knockdown in cancer cells depends on the tumor histotype (Ameln et al., 2011; Andersen et al., 2011; Bordoli et al., 2011; Chan et al., 2009; Kamphues et al., 2012; Lee et al., 2008; Peurala et al., 2012; Su et al., 2012), while our data show a better disease outcome when the tumor stroma is insufficient for *Phd2*. To assess the effect of combined *Phd2* inactivation in cancer cells and stromal cells, we subcutaneously injected scramble and *Phd2*-silenced LLC cells in $R26;Phd2^{+/+}$ and $R26;Phd2^{L/+}$ mice. The efficiency of PHD2 silencing was 65% on both RNA and protein levels (Figure S3D). In vitro, hypoxia, but not *Phd2* silencing, enhanced the expression of VEGF (Figure S3E). In vivo, due to vessel normalization and the subsequent decrease in tumor hypoxia, intratumoral VEGF in $R26;Phd2^{L/+}$ mice was lower than in $R26;Phd2^{+/+}$ mice, regardless of *Phd2* silencing in cancer cells (Figures 3K and S3F). Following doxorubicin treatment, the chemoresponse of both scramble and *Phd2*-silenced LLC tumors was equally improved in $R26;Phd2^{L/+}$ mice (Figure 3L).

These data suggest that systemic inhibition of PHD2 might offer a therapeutic benefit.

Loss of *Phd2* Protects Normal Organs against Side-Toxicity of Chemotherapy

Side-toxicity limits the clinical use of chemotherapeutic drugs. Thus, we wanted to assess the effect of cisplatin and doxorubicin on WT and $Phd2^{+/-}$ kidneys and hearts, respective target organs for drug toxicity. Three days after acute cisplatin administration (20 mg/kg), blood urea and creatinine were 7.9- and 21.9-fold increased in WT mice, but only 4.7 and 4.3 times higher in $Phd2^{+/-}$ mice (Figure 4A). Histological inspection of periodic acid-Schiff (PAS)-stained kidney sections from WT mice revealed severe proximal tubular necrosis and dilatation with formation of protein casts into the lumen, overt destruction of the brush border, and consequent deformations/atrophy of the glomerular structures (Figure 4B). In contrast, the histological morphology of $Phd2^{+/-}$ kidneys was preserved and more comparable to the one of untreated kidneys (Figures 4B and S4A). Transcript levels of kidney injury molecule 1 (*Kim1*) and protein levels of the apoptotic marker-cleaved caspase-3 were strongly induced by cisplatin in WT, but barely in $Phd2^{+/-}$ kidneys (Figures 4C and 4D and Table S3). Consistently, the mean survival after cisplatin was 7 days in $Phd2^{+/-}$ mice, while only 3 days in WT mice (Figure 4E). Upon chronic administration of cisplatin (2.5 mg/kg; 3× per week), only urea, but not creatinine, rose to indicative levels of nephrotoxicity in WT mice, while $Phd2^{+/-}$ mice showed great protection (Figure S4B).

Similarly, WT and $Phd2^{+/-}$ mice were treated with an acute dose of doxorubicin (20 mg/kg). Five days after drug administration, doxorubicin reduced cardiac output by 22.3% in WT mice, while it did not display any effect in $Phd2^{+/-}$ mice (Figure 5A). In doxorubicin-treated WT mice, histological analysis of heart sections revealed disarray and vacuolization of myofibers with excessive collagen deposition, all histopathological signs of cardiomyopathy (Figures 5B and 5C). In $Phd2^{+/-}$ hearts, these features were milder and rarely observed, overall resembling the structure of untreated hearts (Figures 5B and S5A). Creatine

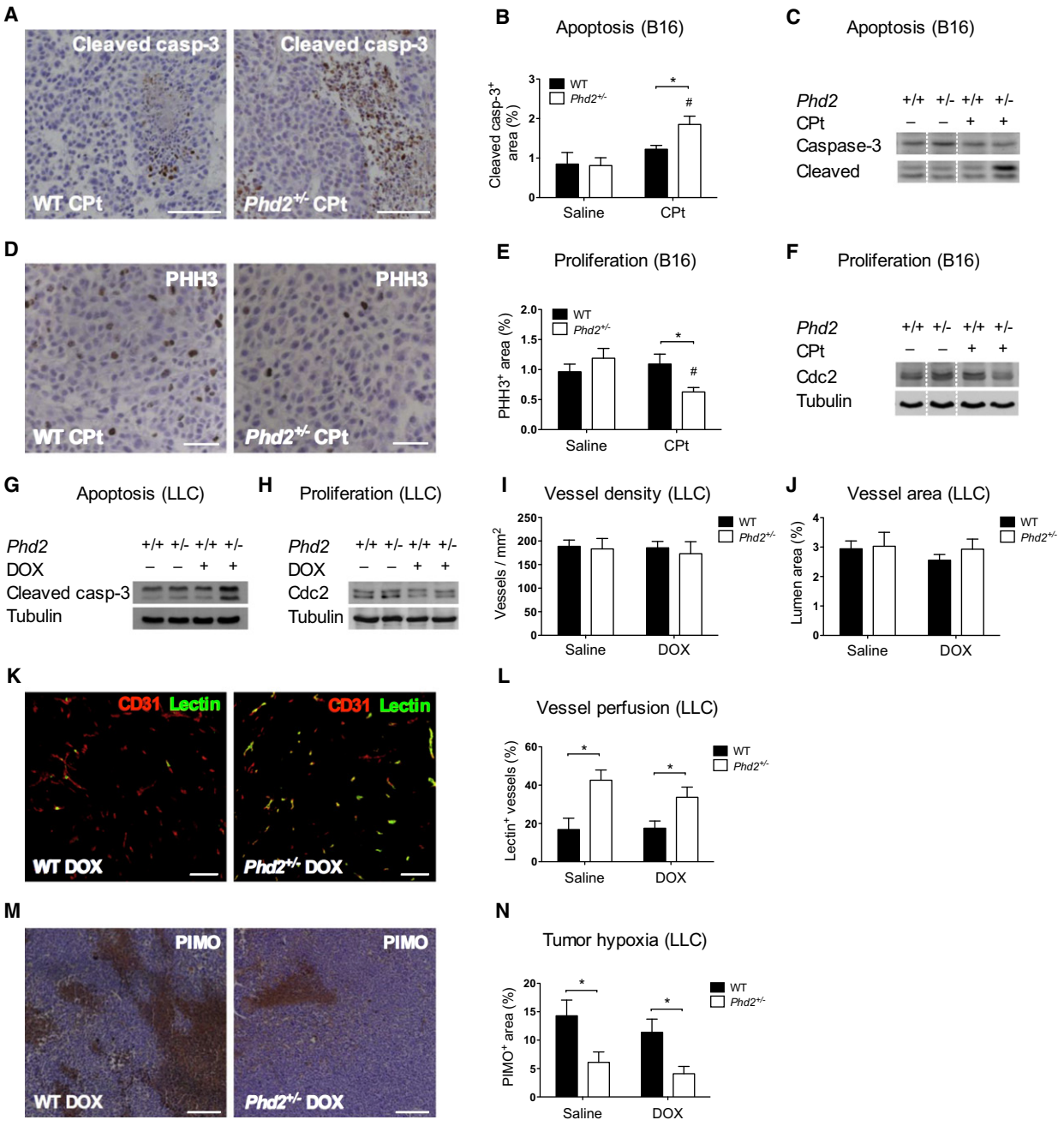

Figure 2. Histological Analysis of Tumors in *Phd2*$^{+/-}$ Mice after Chemotherapy

(A and B) Cleaved caspase-3 staining (A) and morphometric quantification (B) on B16 tumor sections, showing increased tumor apoptosis in *Phd2*$^{+/-}$ mice after CPt (n = 5–6).

(C) Immunoblot for cleaved and total caspase-3, revealing increased tumor apoptosis in *Phd2*$^{+/-}$ mice after CPt (n = 3).

(D and E) Phosphohistone H3 staining (D) and morphometric quantification (E) on B16 tumor sections, showing reduced tumor cell proliferation in *Phd2*$^{+/-}$ mice after CPt (n = 5–6).

(F) Immunoblot for the proliferation marker Cdc2 on untreated and Cpt-treated B16 tumors; tubulin is used as loading control (n = 3).

(G and H) Immunoblot for cleaved caspase-3 (G) and Cdc2 (H) on untreated and DOX-treated LLC tumors (n = 3).

(I and J) Vessel density (I) and vessel area (J) of LLC tumors (n = 6–10).

(K and L) Representative micrographs (K) and morphometric quantification (L) of LLC tumor sections stained for the endothelial marker CD31 (red) and for intravenously injected lectin (green), showing higher vessel perfusion in both untreated and DOX-treated *Phd2*$^{+/-}$ mice (n = 7–9).

(M and N) Pimonidazole (PIMO) staining (M) and morphometric quantification (N) on LLC tumor sections, showing reduced tumor hypoxia in both untreated and DOX-treated *Phd2*$^{+/-}$ mice (n = 7–9).

$^{*}p < 0.05$ versus WT; $^{\#}p < 0.05$ versus saline. Scale bars denote 100 μm in (A), (K), and (M) and 20 μm in (D). All graphs show mean ± SEM. See also Figure S2 and Table S1.

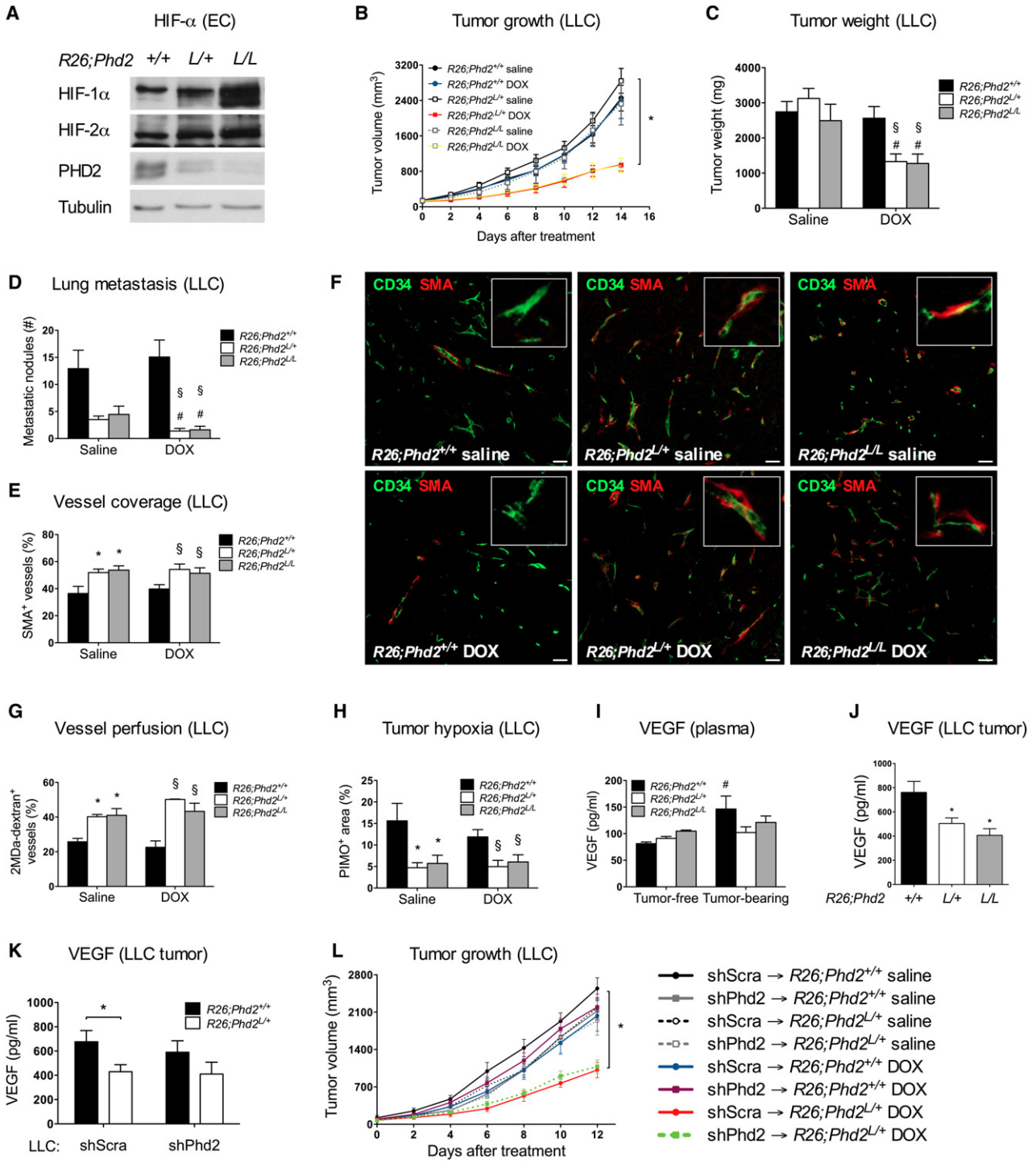

Figure 3. Acute Loss of *Phd2* Enhances Tumor Response to Chemotherapy

(A) Immunoblot for HIF-1α and HIF-2α in WT (*R26;Phd2*$^{+/+}$), *Phd2* haplodeficient (*R26;Phd2*$^{L/+}$), and *Phd2* null (*R26;Phd2*$^{L/L}$) endothelial cells (EC).

(B and C) Reduced LLC tumor growth (B) and weight (C) following DOX (2.5 mg/kg, 3× per week) upon tamoxifen-induced deletion of one (*R26;Phd2*$^{L/+}$) or two (*R26;Phd2*$^{L/L}$) *Phd2* alleles (n = 10–12; *p < 0.05).

(D) Metastasis inhibition in *R26;Phd2*$^{L/+}$ and *R26;Phd2*$^{L/L}$ LLC tumor-bearing mice; lung metastatic nodules were further reduced upon DOX (n = 10–12).

(E and F) Quantification (E) and staining (F) for CD34 (green) and alpha-smooth muscle actin (SMA) (red), revealing increased pericyte coverage of tumor vessels in untreated and DOX-treated *R26;Phd2*$^{L/+}$ and *R26;Phd2*$^{L/L}$ mice. Higher magnification images are shown as insets (n = 6–8).

(G and H) Morphometric quantification of LLC tumor sections stained for the endothelial marker CD31 and intravenously injected 2 MDa dextran-FITC (G) or PIMO (H), showing, respectively, increased tumor vessel perfusion or reduced tumor hypoxia in both untreated and DOX-treated *R26;Phd2*$^{L/+}$ and *R26;Phd2*$^{L/L}$ mice (n = 10–12 or n = 4–6, respectively).

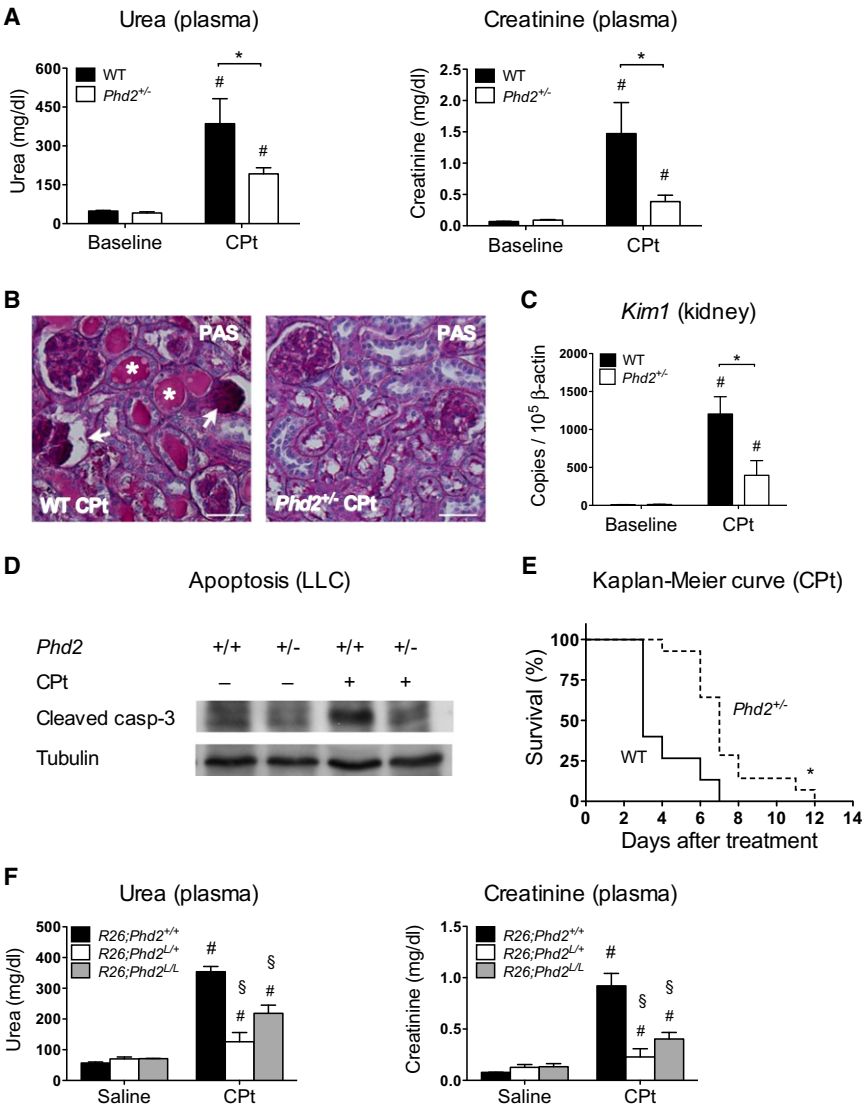

Figure 4. *Phd2* Loss Protects against Cisplatin-Induced Nephrotoxicity

(A) Reduced plasma urea and creatinine in $Phd2^{+/-}$ mice 72 hr post-CPt injection (20 mg/kg; n = 6–10).

(B) PAS staining on kidney sections from CPt-treated mice, revealing severe tubular dilation, protein cast (white asterisks), and detachment of atrophic glomeruli (white arrow) in WT, but not in $Phd2^{+/-}$ mice.

(C) RNA levels of kidney injury molecule 1 (*Kim1*) after CPt (n = 6–10).

(D) Immunoblot for cleaved caspase-3 on kidneys showing protection in $Phd2^{+/-}$ mice against CPt-induced apoptosis.

(E) Kaplan-Meier survival curve, illustrating increased survival of $Phd2^{+/-}$ mice upon acute administration of CPt.

(F) Reduced plasma urea and creatinine levels in CPt-treated $R26;Phd2^{L/+}$ and $R26;Phd2^{L/L}$ mice (n = 5–7; $^{\#}p < 0.05$ versus baseline $R26;Phd2^{+/+}$; $^{\S}p < 0.05$ versus $R26;Phd2^{+/+}$ CPt).

Unless otherwise denoted: $^{*}p < 0.05$ versus WT, $^{\#}p < 0.05$ versus baseline. Scale bars denote 40 μm in (B). All graphs show mean ± SEM. See also Figure S4 and Table S3.

kinase (CK), released in the plasma upon acute cardiac injury, was strongly elevated in WT mice, but 2-fold lower in $Phd2^{+/-}$ mice (Figure 5D). Myocardial death following doxorubicin administration was completely prevented in $Phd2^{+/-}$ mice (Figure 5E and Table S4). Consistently, the mean survival after doxorubicin was 20 days in $Phd2^{+/-}$ mice, while only 5 days in WT mice (Figure 5F). A chronic regimen of doxorubicin as well (2.5 mg/kg; 3× per week) preserved cardiac ejection fraction in $Phd2^{+/-}$ mice (Figure 5G). Gene expression of brain natriuretic peptide (*Bnp*), a marker of chronic heart toxicity, was 35.2% lower in $Phd2^{+/-}$ than WT mice after doxorubicin (Figure 5H).

The protection of healthy organs against chemotherapy can be mainly ascribed to reduced activity of PHD2 in tissue cells, since heterozygous deletion of *Phd2* in EC (and infiltrating leukocytes) did not prevent side-toxicity of cisplatin and doxorubicin (Figures S4C and S5B).

We then assessed the effect of acute deletion of one versus two *Phd2* alleles. To this end, $R26;Phd2^{L/+}$, $R26;Phd2^{L/L}$, and $R26;Phd2^{+/+}$ control mice, pretreated with tamoxifen for 5 days, were injected with an acute dose of cisplatin (20 mg/kg) or doxorubicin (20 mg/kg). Both heterozygous and homozygous deletion of *Phd2* were equally able to prevent renal and cardiac damage, as assessed by lower concentrations of plasma urea, creatinine, and CK in $R26;Phd2^{L/+}$ and $R26;Phd2^{+/+}$ mice after drug administration (Figures 4F and 5I).

Altogether, these results indicate that genetic inactivation of *Phd2* confers protection against chemotherapy-associated nephropathy and cardiomyopathy.

(I) Plasma VEGF levels quantified by ELISA in $R26;Phd2^{+/+}$, $R26;Phd2^{L/+}$, and $R26;Phd2^{L/L}$ LLC tumor-free as well as tumor-bearing mice (n = 5–10; $^{\#}p < 0.05$ versus $R26;Phd2^{+/+}$ tumor-free).

(J) Intratumoral VEGF levels are decreased in $R26;Phd2^{L/+}$ and $R26;Phd2^{L/L}$ mice (n = 6–8).

(K) Intratumoral VEGF levels are decreased in $R26;Phd2^{L/+}$ mice, regardless of *Phd2* silencing in cancer cells (n = 8–10; $^{*}p < 0.05$).

(L) Combined inactivation of *Phd2* in both stroma ($R26;Phd2^{+/+}$ and $R26;Phd2^{L/+}$ mice) and cancer cells (shPhd2) equally enhances LLC tumor response to DOX (2.5 mg/kg, 3× per week) (n = 8–10; $^{*}p < 0.05$).

Unless otherwise denoted: $^{*}p < 0.05$ versus $R26;Phd2^{+/+}$ saline, $^{\#}p < 0.05$ versus saline, $^{\S}p < 0.05$ versus $R26;Phd2^{+/+}$ DOX. Scale bars denote 50 μm in (F). All graphs show mean ± SEM. See also Figure S3 and Table S2.

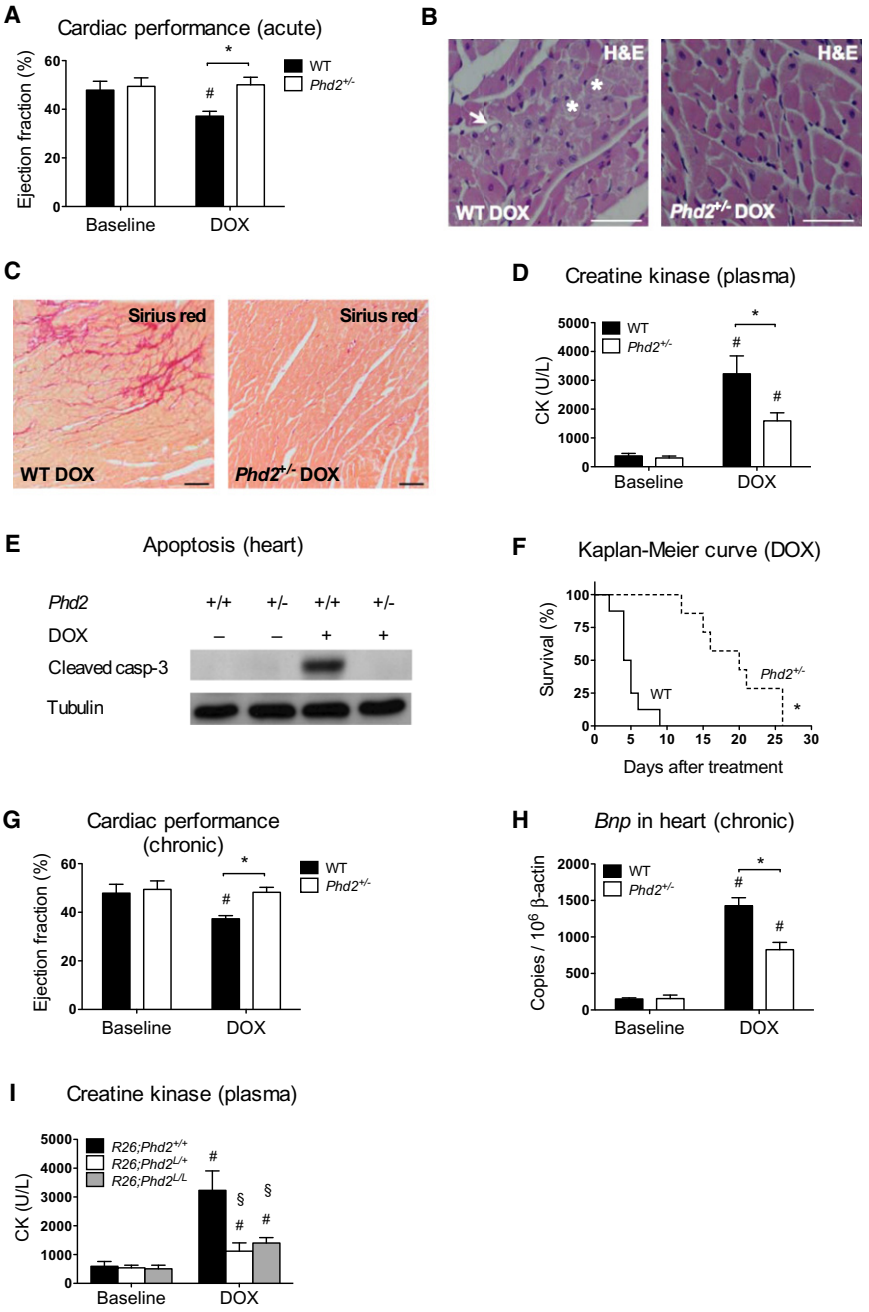

Figure 5. *Phd2* Loss Protects against Doxorubicin-Induced Cardiotoxicity

(A) B-mode measurement of left ventricular function, revealing unaltered ejection fraction in $Phd2^{+/-}$ mice 5 days after acute administration of DOX (20 mg/kg; n = 7–11).

(B) H&E-staining on DOX-treated heart sections reveals extensive cytoplasmic vacuolization (white arrow), myofibrillar loss, and cell death (white asterisks) in WT, but not in $Phd2^{+/-}$ mice.

(C) Sirius red staining on DOX-treated heart sections identifies extensive fibrotic areas in WT, but not in $Phd2^{+/-}$ mice.

(D) Increased plasma creatine kinase (CK) by DOX is prevented in $Phd2^{+/-}$ mice (n = 5–7).

(E) Immunoblot for cleaved caspase-3 on hearts showing prevention of DOX-induced apoptotis in $Phd2^{+/-}$ mice.

(F) Kaplan-Meier curve, illustrating increased survival of $Phd2^{+/-}$ mice upon acute administration of DOX (n = 7–8; *p < 0.001 versus WT).

(G) B-mode measurement of left ventricular function in $Phd2^{+/-}$ and WT mice 1 month after chronic treatment (2.5 mg/kg; 3× per week) with DOX (n = 30; *p < 0.001; #p < 0.001 versus baseline).

(H) RNA levels of brain natriuretic peptide (*Bnp*) in heart after chronic administration of DOX (n = 9–11).

(I) Plasma CK values upon acute DOX treatment in tamoxifen-treated in *R26;Phd2*$^{+/+}$, *R26;Phd2*$^{L/+}$, and *R26;Phd2*$^{L/L}$ mice (n = 5–7; #p < 0.05 versus baseline *R26;Phd2*$^{+/+}$; §p < 0.05 versus *R26;Phd2*$^{+/+}$ DOX).

Unless otherwise denoted: *p < 0.05 versus WT, #p < 0.05 versus baseline. Scale bars denote 20 μm in (B) and (C). All graphs show mean ± SEM. See also Figure S5 and Table S4.

Loss of *Phd2* Mounts an Antioxidative Response in Normal Organs

The toxicity of cisplatin and doxorubicin on quiescent and healthy organs has been, in part, ascribed to oxidative stress formation (Berthiaume and Wallace, 2007; Pabla and Dong, 2008). We therefore assessed the burst of ROS after chemotherapy by staining kidney and heart sections for 8-hydroxy deoxyguanosine (8-OHdG), a marker of oxidative DNA damage. Acute cisplatin administration raised the number of 8-OHdG$^+$ nuclei in WT kidneys to 52.3%, while only to 35% in $Phd2^{+/-}$ kidneys (Figures 6A and 6B). 8-OHdG$^+$ nuclei were undetectable at baseline in both genotypes (Figure S6A). Similarly, both acute and chronic administration of doxorubicin resulted in reduced oxidative damage in $Phd2^{+/-}$ versus WT hearts (Figures 6C–6E). 8-OHdG$^+$ nuclei in baseline hearts were similar in both genotypes (Figures S6B and S6C). When treated with acute regimens of doxorubicin or cisplatin, RNA, protein levels, and activity of primary antioxidative enzymes (AOE), such as superoxide dismutase 1 (*Sod1*), superoxide dismutase 2 (*Sod2*), catalase (*Cat*), and glutathione peroxidase 1 (*Gpx1*), were significantly higher in $Phd2^{+/-}$ than in WT organs (Figures 6F–6H and Tables S5 and S6). Baseline levels and activity of these enzymes were similar in both genotypes (not shown). Administration of the ROS scavenger Mn(III)tetrakis(4-benzoic acid)porphyrin (MnTBAP) greatly prevented the induction of AOE in $Phd2^{+/-}$ hearts after doxorubicin, indicating that ROS production by chemotherapy is necessary to trigger this detoxification response (Figure 6I). Pharmacological inhibition of these AOE in combination with doxorubicin completely abrogated the cardiac protection conferred by loss of *Phd2* (Figure 6J).

We then assessed whether the nonspecific prolyl hydroxylase inhibitor dimethyloxaloylglycine (DMOG) could offer a similar cardiac protection as genetic inactivation of *Phd2*. When measuring plasma CK as readout of toxicity, DMOG-treated WT mice displayed a 53% reduction of CK release after doxorubicin (Figure 6K). From a molecular point of view, DMOG alone did not induce AOE upregulation, in line with our observations in $Phd2^{+/-}$ mice at baseline. However, the combination of DMOG and doxorubicin enhanced the expression of *Cat*, *Sod1*, *Sod2*, and *Gpx1*, consistent with the fact that an oxidative challenge is required to initiate the detoxification response (Figure 6L).

We also evaluated the biological consequences of reduced PHD2 activity on ROS homeostasis in LLC cancer cells, where the cytostatic effect of these drugs is primarily linked to cell proliferation (not shown). Silencing of *Phd2* did not affect the expression of AOE either in vitro or in vivo: neither did it affect ROS induction (Figures S6D–S6G). Consistently, in vitro cell death in response to doxorubicin was comparable in both scramble and *Phd2*-silenced LLC (Figure S6H).

Thus, a reduction of PHD2 triggers effective antioxidative responses in normal organs, but not in tumors, in response to chemotherapy.

The Antioxidative Response by Loss of *Phd2* Is HIF-1 and HIF-2 Dependent

The AOE upregulated in $Phd2^{+/-}$ organs are HIF downstream targets (Scortegagna et al., 2003). To assess HIF transcriptional activity in WT and $Phd2^{+/-}$ hearts at baseline and after doxorubicin, we used an adenoassociated virus serotype-9 (AAV9) carrying a HIF-responsive firefly luciferase reporter (Figure 7A). HIF activity was comparable in both genotypes at baseline. However, 24 hr after doxorubicin administration, HIF activity was 5.4 times higher in WT hearts, but 9.8 times higher in $Phd2^{+/-}$ hearts (Figure 7A). This effect was specific and not secondary to hypoxia, since the constitutive cytomegalovirus (CMV) promoter was not differentially regulated and we were not able to detect any hypoxic regions in response to doxorubicin (Figure S7A and not shown). Similar results were obtained in kidneys, where HIF activity 24 hr after a bolus of cisplatin was 8.1-fold increased in WT mice, but 13.5-fold increased in $Phd2^{+/-}$ mice (Figure 7B).

To assess the contribution of HIF-1α versus HIF-2α, we intercrossed $Phd2^{+/-}$ mice with $Hif1a^{+/-}$ or $Hif2a^{+/-}$ mice, displaying about 50% reduction in *Hif1a* or *Hif2a*, respectively (Figures S7B and S7C). Heterozygous deficiency of either *Hif1a* or *Hif2a* in $Phd2^{+/-}$ mice abrogated the upregulation of *Sod1*, *Sod2*, *Cat*, and *Gpx1* after doxorubicin (Figures 7C and 7D). In vitro, both HIF-1α and HIF-2α were more abundant in $Phd2^{+/-}$ cardiomyocytes compared to WT and accumulated to even higher levels in $Phd2^{-/-}$ cardiomyocytes (Figure 7E and Table S7). In response to doxorubicin, both HIFs were slightly higher in WT cardiomyocytes, but they were more potently induced in $Phd2^{+/-}$ and in $Phd2^{-/-}$ cells up to comparable levels (Figure 7E and Table S7).

In order to block simultaneously HIF-1 and HIF-2, we treated WT and $Phd2^{+/-}$ mice with chetomin, which disrupts the interaction of the transcriptional coactivator p300 with the alpha subunit of HIF (Kung et al., 2004). Administration of chetomin prevented the induction of *Sod1*, *Sod2*, *Cat*, and *Gpx1* and completely abrogated the protection against oxidative stress and tissue damage conferred by *Phd2* haplodeficiency in response to doxorubicin (Figures 8A–8C), supporting that both HIFs are responsible for the chemoprotection in $Phd2^{+/-}$ mice.

DISCUSSION

During the last decade, much progress has been made in increasing the arsenal and selectivity of anticancer drugs. However, side effects and resistance to therapy still remain major issues (Berthiaume and Wallace, 2007; Pabla and Dong, 2008). Based on previous research (Mazzone et al., 2009), we now describe PHD2 as a potential and promising target, not only to improve delivery of cytotoxic drugs selectively to the tumor, but also to protect normal organ functions from side-toxicity of chemotherapy. From a biological point of view, two distinct mechanisms underlie these different phenomena. In tumors, on one hand, we show that acute deletion of one or two *Phd2* alleles in stromal cells increases tumor vessel perfusion and thus allows doxorubicin and cisplatin to better reach the tumor, regardless of *Phd2* targeting in cancer cells. Together with the inhibition of metastasis, PHD2 inactivation provides a potent antitumor effect when combined with conventional chemotherapeutic regimens (Figure 8D, left panel). In healthy organs, on the other hand, reduced activity of PHD2 in hearts and kidneys amplifies the antioxidative response and thus counters the oxidative burst and subsequent tissue damage caused by doxorubicin and cisplatin (Figure 8D, right panel).

Previous studies have shown that VEGF(R) blockade promotes a transient window of tumor vessel normalization in which the chemo- and radio-response of the tumor is enhanced (Goel et al., 2011; Winkler et al., 2004). Beyond this "normalization window," VEGF blockade leads to vessel pruning, which might increase hypoxia and fuel a shift to malignancy, together with an overall reduction of drug delivery and tumor uptake (Loges et al., 2009). In addition, resistance mechanisms are evoked by the antiangiogenic treatment itself (Loges et al., 2009). By using different genetic tools, we show that reduced activity of PHD2 in EC normalizes the tumor vasculature, not vessel numbers, and increases drug efficiency. This effect is similar and preserved until the end stage of the disease if *Phd2* is inactivated either before or after tumor onset or following systemic inactivation of one or two *Phd2* alleles. Moreover, chemotherapeutic drugs in $Phd2^{+/-}$ mice have a synergic effect on metastasis inhibition. Finally, $Phd2^{+/-}$ vessels have improved functionality prior to and postchemotherapy, altogether suggesting the absence of resistance modes. Nevertheless, we cannot formally exclude that PHD2 might affect tumor-stromal interactions that confer protection on cancer cells from the cytotoxic effect of anticancer agents (Provenzano et al., 2012; Nakasone et al., 2012). A deletion of *Phd2* in the host stroma may alter its interactions with cancer cells, resulting in an unfavorable microenvironment that could render tumor cells more sensitive to drug treatment.

Phd2 silencing in cancer cells can display both a pro- and antitumoral effect, depending on the cellular context (Ameln et al., 2011; Andersen et al., 2011; Bordoli et al., 2011; Chan et al., 2009; Kamphues et al., 2012; Lee et al., 2008; Peurala et al., 2012; Su et al., 2012). However, there are more tumor

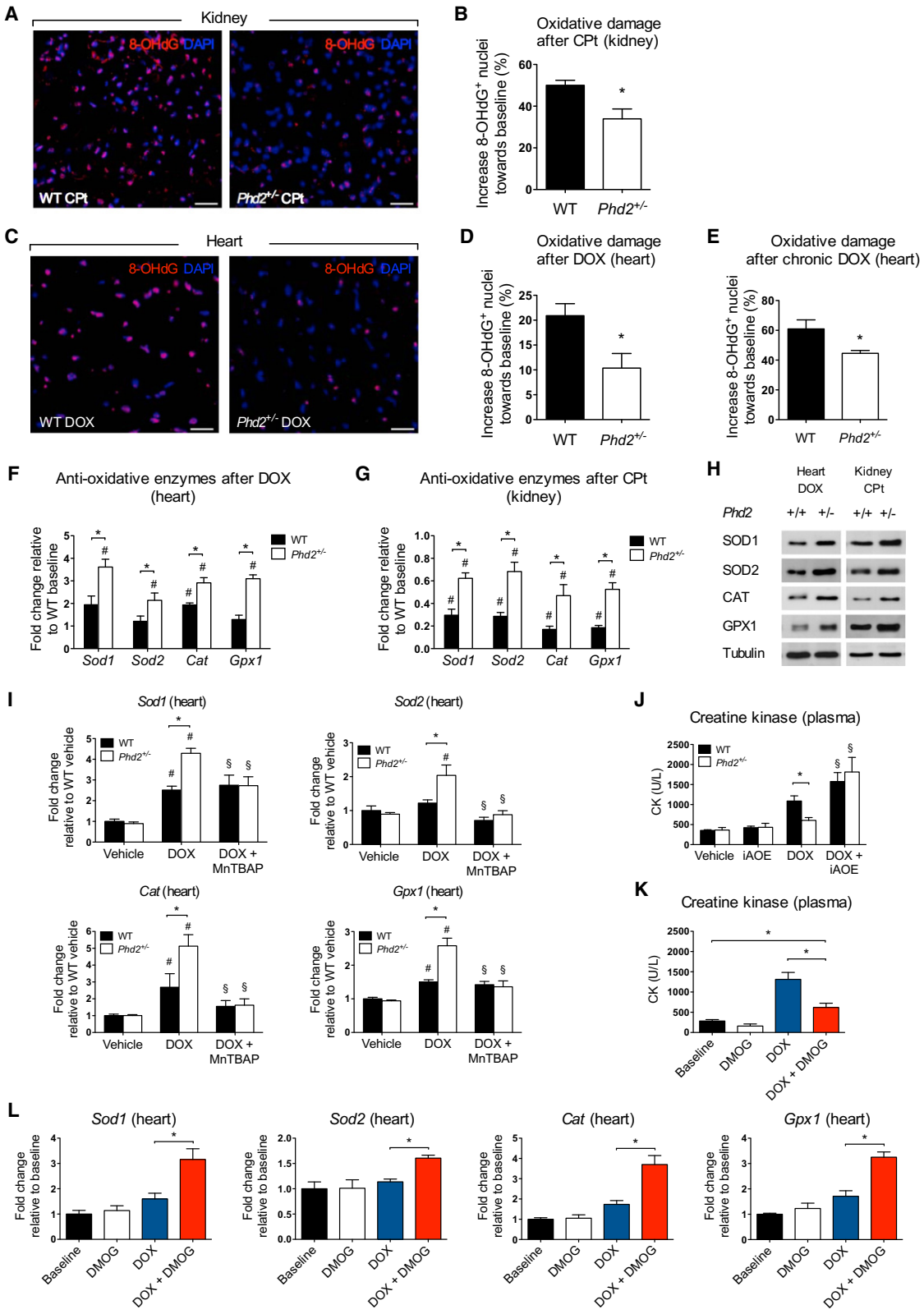

Figure 6. *Phd2* Loss Favors an Antioxidative Response in Normal Organs

(A–D) Representative micrographs (A,C) and morphometric quantification (B,D) of 8-hydroxy deoxyguanosine (8-OHdG; red) positive nuclei in kidney sections 72 hr after acute administration of CPt (20 mg/kg) or in heart sections 5 days after acute administration of DOX (20 mg/kg), respectively; DAPI (blue) was used for nuclear localization (n = 5).

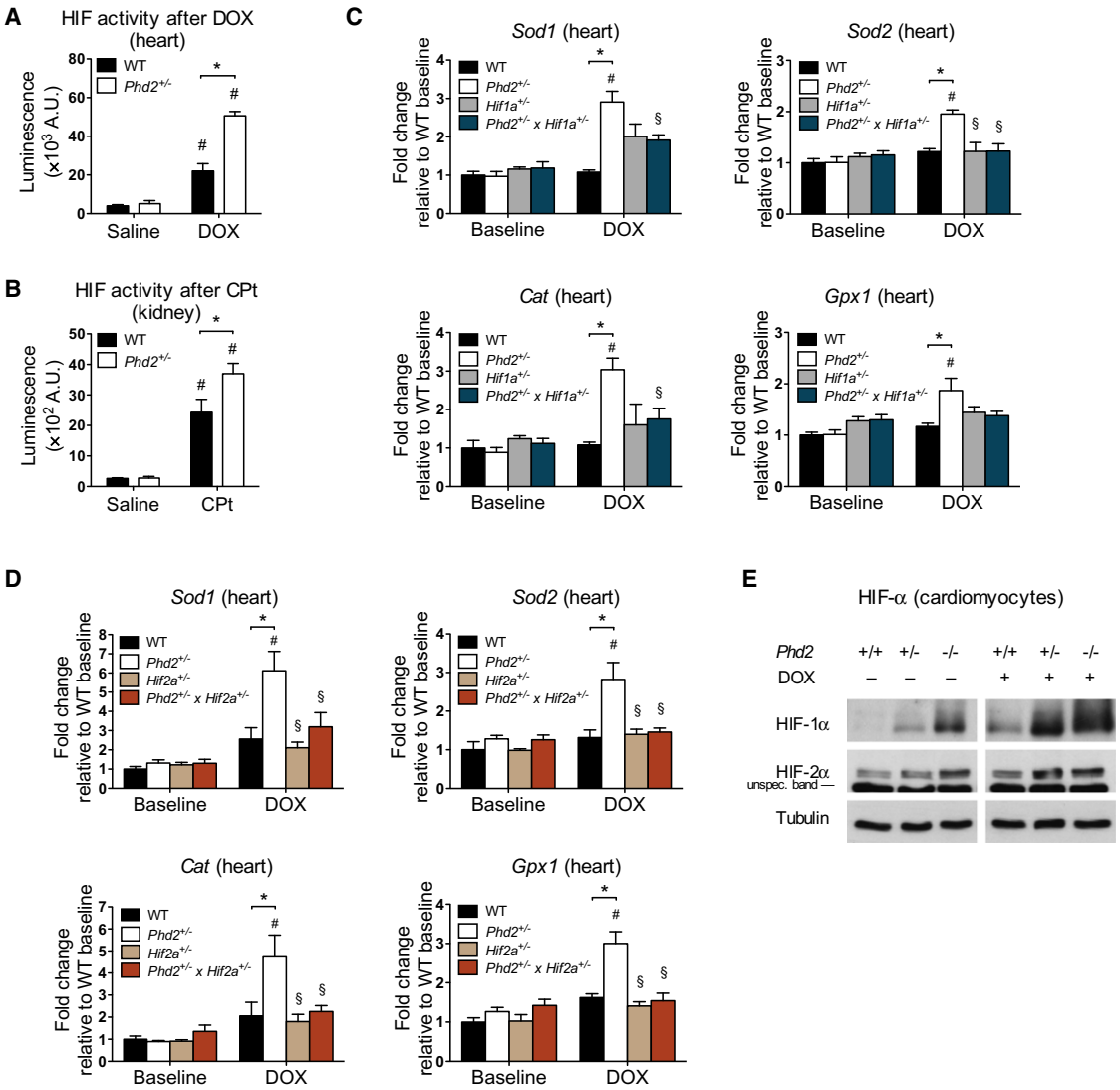

Figure 7. Chemoprotection of Normal Organs by *Phd2* Loss Requires HIF-1 and HIF-2

(A and B) HIF-reporter luciferase assay, showing enhanced HIF activity upon chemotherapy in $Phd2^{+/-}$ hearts (A) and kidneys (B) (n = 4).

(C and D) Either *Hif1a* (C) or *Hif2a* (D) heterozygosity prevents the transcriptional induction of AOE in $Phd2^{+/-}$ mice upon DOX treatment (n = 5–10).

(E) Immunoblot for HIF-1α and HIF-2α in untreated and DOX-treated WT, $Phd2^{+/-}$, and $Phd2^{-/-}$ cardiomyocytes.

*p < 0.05 versus WT, #p < 0.05 versus baseline, §p < 0.05 versus $Phd2^{+/-}$ DOX. All graphs show mean ± SEM. See also Figure S7 and Table S7.

types that overexpress *Phd2* compared to their normal histological counterpart than tumor types that underexpress this gene, thus indicating *Phd2* as an oncogene more than an oncosuppressor (Ameln et al., 2011). For this reason, simultaneous inactivation of *Phd2* in both tumor stroma and cancer cells remained enigmatic. Our data show that tumors generated by *Phd2* hypomorphic LLC cells still display an advantageous response to chemotherapy when the tumor is embedded in

(E) 8-OHdG positive nuclei are significantly reduced in $Phd2^{+/-}$ hearts under a chronic regimen of DOX (2.5 mg/kg; 3× per week; n = 4–8; *p < 0.05).

(F–H) Enhanced expression of antioxidative enzymes (AOE) in $Phd2^{+/-}$ hearts (F) and kidneys (G) after chemotherapy, both at the RNA (F and G; n = 6) and protein (H; n = 3) levels.

(I) RNA levels of AOE in DOX-treated $Phd2^{+/-}$ mice upon administration of the ROS scavenger MnTBAP (n = 3–5; #p < 0.05 versus WT vehicle).

(J) Plasma CK upon combined treatment with DOX and AOE inhibitors (n = 3–6).

(K) Treatment of WT mice with the nonspecific PHD2 inhibitor DMOG prevents the increase of plasma CK after DOX (n = 5–6).

(L) Combined administration of DMOG and DOX strongly upregulates AOE transcript levels in WT hearts (n = 5–6).

Unless otherwise denoted: *p < 0.05 versus WT, #p < 0.05 versus WT baseline (not shown) or vehicle, §p < 0.05 versus $Phd2^{+/-}$ DOX. Scale bars denote 20 μm in (A) and (C). All graphs show mean ± SEM. See also Figure S6 and Tables S5 and S6.

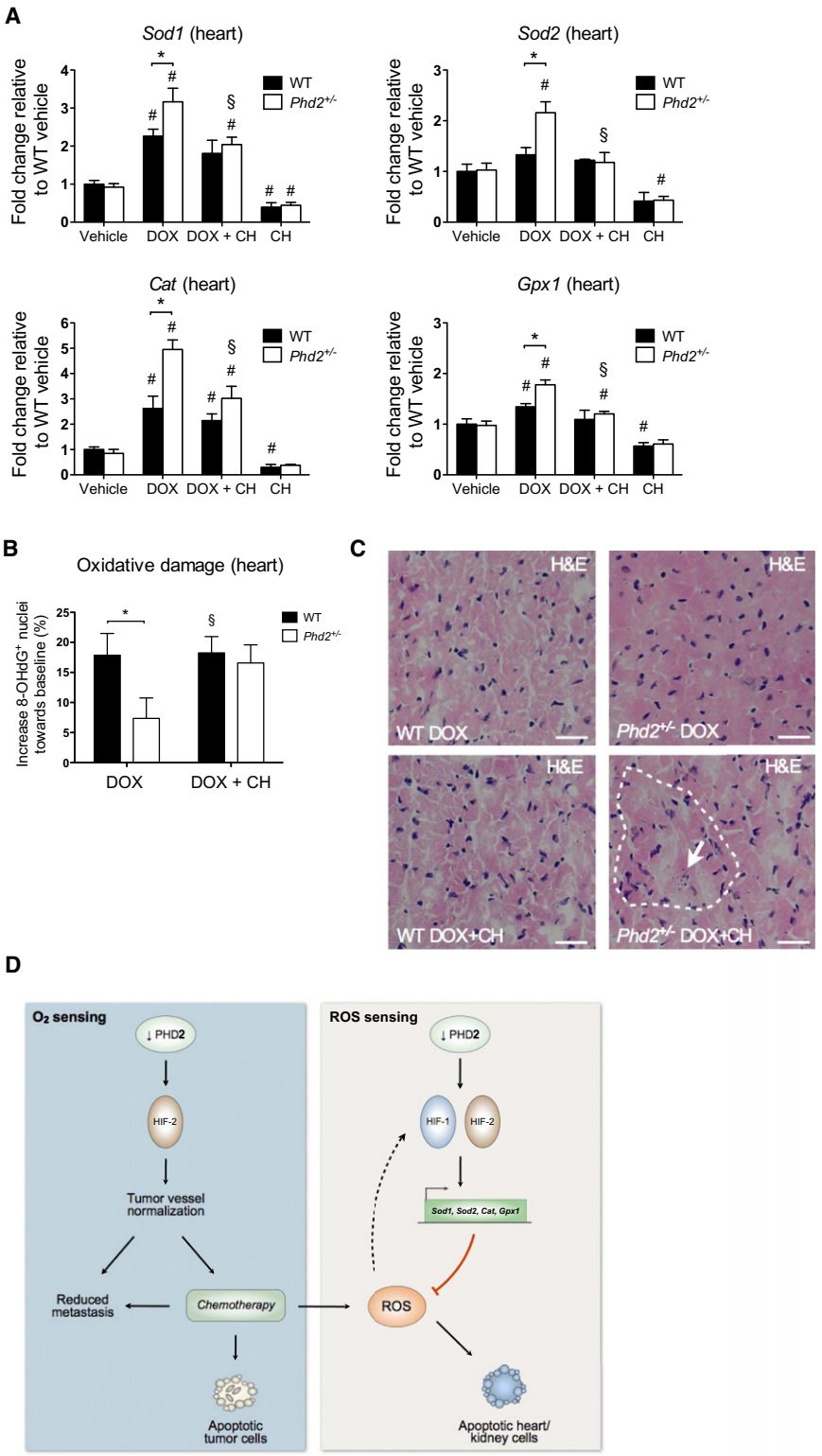

Figure 8. HIF-Inhibition Abrogates Chemoprotection in *Phd2*$^{+/-}$ Mice

(A) RNA levels of AOE in WT and *Phd2*$^{+/-}$ hearts upon combined treatment with DOX and the HIF-inhibitor chetomin (CH; n = 6).

(B) Morphometric quantification of 8-OHdG^{+} nuclei, showing increased oxidative stress in *Phd2*$^{+/-}$ mice upon combined DOX and CH treatment (n = 5).

(C) H&E-stained heart sections show increased myofiber disarray (dotted line) and apoptotic features (arrow) in *Phd2*$^{+/-}$ mice after combined treatment of DOX and CH.

(D) Acting as an oxygen-sensitive enzyme, reduced activity of PHD2 in EC promotes tumor vessel normalization in a HIF-2α-dependent manner, thus optimizing the delivery of chemotherapeutic drugs to the tumor, increasing their antitumor and antimetastatic effects (left panel). In healthy organs, the overall prolyl hydroxylase activity is hampered by chemotherapy-induced reactive oxygen species (ROS), resulting in HIF-1α and HIF-2α stabilization and subsequent transcription of antioxidative defenses (*Sod1, Sod2, Cat*, and *Gpx1*). Genetic deletion of *Phd2* reduces the threshold of HIFs activation and thus favors this feedback loop, which promptly counters oxidative damage and prevents organ failure and tissue demise (right panel). Targeting PHD2 might therefore offer a double advantage in the treatment of oncological diseases.

*p < 0.05 versus WT, #p < 0.05 versus baseline, §p < 0.05 versus *Phd2*$^{+/-}$ DOX. Scale bars denote 100 μm in (C). All graphs show mean ± SEM.

a *Phd2*-deficient environment, suggesting that systemic inhibition of PHD2 might offer beneficial effects in cancer treatment. Further studies are needed to extend these findings to different tumor cell types.

PHD2 inactivation also prevented cardiac and renal toxicity derived by chemotherapy-induced ROS. Inactivation of PHDs predisposes responses to hypoxia and preconditioning stimuli (Aragonés et al., 2009; Eckle et al., 2008; Huang et al., 2008; Hyvärinen et al., 2010; Mazzone et al., 2009; Takeda et al., 2011). Indeed, oxygen consumption in hypoxia is associated with generation of ROS that peaks after tissue reoxygenation; stabilization of HIF-1α and/or HIF-2α have been associated with transcription of antioxidative defenses that protect the cell from oxidative damage (Date et al., 2005; Lee et al., 1997; Martin et al., 2005; Mukhopadhyay et al., 2000; Scortegagna et al., 2003). However, when the production of ROS overwhelms the detoxification capacity of the cell, excessive oxidative damage leads to cell death (Aragonés et al., 2008; Minotti et al., 2004; Shokolenko et al., 2009; Unnikrishnan et al., 2009). The same phenomenon occurs during treatment with doxorubicin and cisplatin (Berthiaume and Wallace, 2007; Pabla and Dong, 2008).

The current study suggests that an initial burst of ROS production by chemotherapeutic drugs is required to stabilize both HIF-1α and HIF-2α and to promote their activity in normoxic conditions. Indeed, when ROS are increased, iron oxidation results in the inactivation of prolyl hydroxylase activity, since this metal is an essential cofactor for these enzymes (Gerald et al., 2004). This feedback loop provides a built-in safety mechanism to diminish tissue damage. *Phd2* (haplo)deficiency decreases the threshold of HIF activation and favors the transcription of antioxidative defenses that further limit the abundance of ROS. A reduction of prolyl hydroxylase activity by chemotherapy-associated ROS production will also trigger the same detoxification program in WT organs, but less efficiently than in *Phd2* (haplo)deficient organs. In other words, by rendering the organs better preadapted to oxidative stress, (haplo)deficiency of *Phd2* promptly counteracts ROS-induced tissue damage. These findings unravel a mechanism for ROS homeostasis by PHD2, which is independent of hypoxia, and implies a relevance of PHD2 in other oxidative stress-related pathophysiological conditions, such as neurodegenerative disorders, diabetes, and aging (Fraisl et al., 2009).

Our data indicate that the involvement of PHD2 in response to chemotherapeutic drugs is highly context and cell-type dependent, since *Phd2* silencing in proliferating cancer cells did not affect AOE in response to doxorubicin: neither did it modify ROS production. However, the factors conferring cell specificity to this response need to be defined. From a therapeutic point of view, our findings support the idea that systemic inhibition of PHD2 might offer chemoprotection of normal organs without promoting chemoresistance in cancer cells.

In our previous study, we show that HIF-2α is mainly responsible for $Phd2^{+/-}$ EC quiescence/normalization (Mazzone et al., 2009); in this study, we show that both HIF-1α and HIF-2α are involved in the detoxification program in $Phd2^{+/-}$ organs. Both HIFs have been previously reported as upstream regulators of an antioxidative response in different cell types (Bertout et al., 2009; Mukhopadhyay et al., 2000; Scortegagna et al., 2003). Genetic inactivation of *Hif2a* reduced the levels of *Sod1*, *Sod2*, *Cat*, and *Gpx1* and resulted in multiple organ failure in developing embryos and neonates (Scortegagna et al., 2003). However, *Phd2* inactivation will lead to simultaneous accumulation of both HIF isoforms, representing a different scenario from the one described in previous studies, showing genetic deletion (or silencing) of *Hif1a* or *Hif2a* (Bertout et al., 2009; Scortegagna et al., 2003; Vengellur et al., 2003, 2011). Overall, the involvement of HIF in favoring tumor vessel normalization and limiting the undesired effects of chemotherapy warrants some caution for considerate use of HIF inhibitors for cancer therapy (Semenza, 2003).

Finally, heterozygous and homozygous deletion of *Phd2* comparably sensitizes the tumor to chemotherapeutic drugs and minimizes their adverse effects. From a molecular point of view, HIF-2α (the main driver of vessel normalization) was higher, but equally elevated in both $Phd2^{+/-}$ and $Phd2^{-/-}$ EC. This is likely due to compensatory mechanisms in *Phd2* null cells, where *Phd3* upregulation might tune down to the heterozygous levels the genetic response triggered by complete loss of *Phd2*, as reported during embryo development (Minamishima et al., 2009). In cardiomyocytes, despite a dose-dependent effect of heterozygous versus homozygous *Phd2* deletion on HIF-1α and HIF-2α stabilization at baseline, in response to doxorubicin, both HIFs reached their plateau in $Phd2^{+/-}$ and $Phd2^{-/-}$ cells, thus displaying a comparable antioxidative response.

To date, PHD2-specific inhibitors are not commercially available, although several screening platforms have been established (Fraisl et al., 2009). It will be clinically relevant to validate these drugs in mouse models of cancer in combination with chemotherapy. At this stage, our study provides insight on how PHD2 can regulate drug delivery to the tumor by sensing oxygen availability and readapting vessel perfusion and can counter the onset of chemotherapy-associated side-toxicity by working as a gatekeeper for ROS production.

EXPERIMENTAL PROCEDURES

More detailed methods can be found in the Supplemental Information.

Syngeneic Tumor Models

10^6 B16F10.9 melanoma (B16) cells or 10^6 Lewis lung carcinoma (LLC) cells were injected subcutaneously. Tumor volumes were measured 3× per week with a caliper and calculated using the formula: $V = \pi \times [\text{width}^2 \times \text{length}] / 6$. At an average of 100 mm^3, mice were randomized for intraperitoneal (i.p.) administration (2.5 mg/kg; 3× per week) of cisplatin (CPt) or doxorubicin (DOX) in B16 or LLC tumor-bearing mice, respectively. In tumor experiments using the $Rosa26^{CreERT2}$ deleter, tamoxifen treatment (1 mg/mouse/day i.p. for 5 consecutive days) was started on the day of cancer cell injection. Housing and all experimental animal procedures were approved by the Institutional Animal Care and Research Advisory Committee of the KU Leuven.

Cisplatin Quantification

The CPt in B16 tumors was quantified by inductively coupled plasma mass spectrometry (ICP820-MS, Varian, USA) or by immunohistochemical staining against CPt DNA-adducts (NKI-159; a gift of Dr. B. Floot, Netherlands Cancer Institute).

Tumor Interstitial Fluid Pressure

Tumor interstitial fluid pressure was evaluated in the central cystic tumor area of subcutaneous LLC tumors using the "wick-in-needle" technique (Hofmann et al., 2006).

Acute or Chronic Doxorubicin Cardiotoxicity

Tumor-free mice were injected with a single dose of 20 mg/kg DOX (i.p.) and assessed for cardiotoxicity after 5 days or with 2.5 mg/kg DOX (i.p.) three times a week for a total of 4 weeks, respectively.

Acute or Chronic Cisplatin Nephrotoxicity

Tumor-free mice were injected with a single dose of 20 mg/kg CPt (i.p.) and assessed for renal toxicity after 3 days or with 2.5 mg/kg CPt (i.p.) three times a week for a total of 4 weeks, respectively.

HIF Activity In Vivo

The adenovirus-associated virus 9 (AAV9) HIF reporter plasmid (AAV9-HRE-LUC) contains a minimal promoter fused to 9 copies of hypoxia-responsive elements (HRE) followed by the firefly luciferase (LUC)(Aragonés et al., 2001) in pSubCMV-WPRE (Paterna et al., 2000). AAV9 particles were generated as previously described (Anisimov et al., 2009). A dose of 0.25×10^{11} viral genomic copies of AAV9-HRE-LUC or the control AAV9-CMV-LUC were injected in the tail vein 3 days before administration of 20 mg/kg DOX or CPt.

Immunoblot and Immunochemistry

Protein extraction was performed using RIPA (50 mM Tris HCl pH 8, 150 mM NaCl, 1% Triton X-100, 0.1% SDS, 0.5% sodium deoxycolate). All methods for histology and immunostainings have been described before (Mazzone et al., 2009).

QRT-PCR

Quantitative RT-PCR (QRT-PCR) was performed as described (Fischer et al., 2007). The Assay ID (Applied Biosystems) or the sequence of primers and probes (when homemade) are listed in the Supplement Experimental Procedures.

Hypoxia and Tumor Perfusion

Tumor hypoxia was detected as before (Mazzone et al., 2009). Tumor perfusion was assessed by injecting intravenously 0.05 mg lectin-FITC (*Lycopersicon esculentum*; Vector Laboratories) or 5 mg high molecular weight (2 MDa) dextran-FITC (Sigma).

Statistics

Data represent mean ± SEM of representative experiments. Statistical significance was calculated by a two-tailed unpaired t test for two data sets and ANOVA followed by a Bonferroni post hoc test for multiple data sets using Prism (GraphPad, Inc.), with $p < 0.05$ considered statistically significant.

SUPPLEMENTAL INFORMATION

Supplemental Information includes seven figures, seven tables, and Supplemental Experimental Procedures and can be found with this article online at http://dx.doi.org/10.1016/j.ccr.2012.06.028.

ACKNOWLEDGMENTS

The authors thank J. Serneels and B. Das for technical assistance. This work was supported by grants from FWO (G.0718.10N) and Stichting tegen Kanker (2010-169). R.L.O., A.-T.H., and V.F. are granted by FWO.

Received: October 12, 2011
Revised: May 8, 2012
Accepted: June 26, 2012
Published: August 13, 2012

REFERENCES

Ameln, A.K., Muschter, A., Mamlouk, S., Kalucka, J., Prade, I., Franke, K., Rezaei, M., Poitz, D.M., Breier, G., and Wielockx, B. (2011). Inhibition of HIF prolyl hydroxylase-2 blocks tumor growth in mice through the antiproliferative activity of TGFβ. Cancer Res. *71*, 3306–3316.

Andersen, S., Donnem, T., Stenvold, H., Al-Saad, S., Al-Shibli, K., Busund, L.T., and Bremnes, R.M. (2011). Overexpression of the HIF hydroxylases PHD1, PHD2, PHD3 and FIH are individually and collectively unfavorable prognosticators for NSCLC survival. PLoS ONE *6*, e23847.

Anisimov, A., Alitalo, A., Korpisalo, P., Soronen, J., Kaijalainen, S., Leppänen, V.M., Jeltsch, M., Ylä-Herttuala, S., and Alitalo, K. (2009). Activated forms of VEGF-C and VEGF-D provide improved vascular function in skeletal muscle. Circ. Res. *104*, 1302–1312.

Anscher, M.S., Chen, L., Rabbani, Z., Kang, S., Larrier, N., Huang, H., Samulski, T.V., Dewhirst, M.W., Brizel, D.M., Folz, R.J., and Vujaskovic, Z. (2005). Recent progress in defining mechanisms and potential targets for prevention of normal tissue injury after radiation therapy. Int. J. Radiat. Oncol. Biol. Phys. *62*, 255–259.

Aragonés, J., Jones, D.R., Martin, S., San Juan, M.A., Alfranca, A., Vidal, F., Vara, A., Mérida, I., and Landázuri, M.O. (2001). Evidence for the involvement of diacylglycerol kinase in the activation of hypoxia-inducible transcription factor 1 by low oxygen tension. J. Biol. Chem. *276*, 10548–10555.

Aragonés, J., Schneider, M., Van Geyte, K., Fraisl, P., Dresselaers, T., Mazzone, M., Dirkx, R., Zacchigna, S., Lemieux, H., Jeoung, N.H., et al. (2008). Deficiency or inhibition of oxygen sensor Phd1 induces hypoxia tolerance by reprogramming basal metabolism. Nat. Genet. *40*, 170–180.

Aragonés, J., Fraisl, P., Baes, M., and Carmeliet, P. (2009). Oxygen sensors at the crossroad of metabolism. Cell Metab. *9*, 11–22.

Berthiaume, J.M., and Wallace, K.B. (2007). Adriamycin-induced oxidative mitochondrial cardiotoxicity. Cell Biol. Toxicol. *23*, 15–25.

Bertout, J.A., Majmundar, A.J., Gordan, J.D., Lam, J.C., Ditsworth, D., Keith, B., Brown, E.J., Nathanson, K.L., and Simon, M.C. (2009). HIF2alpha inhibition promotes p53 pathway activity, tumor cell death, and radiation responses. Proc. Natl. Acad. Sci. USA *106*, 14391–14396.

Bordoli, M.R., Stiehl, D.P., Borsig, L., Kristiansen, G., Hausladen, S., Schraml, P., Wenger, R.H., and Camenisch, G. (2011). Prolyl-4-hydroxylase PHD2- and hypoxia-inducible factor 2-dependent regulation of amphiregulin contributes to breast tumorigenesis. Oncogene *30*, 548–560.

Carmeliet, P., and Jain, R.K. (2011). Principles and mechanisms of vessel normalization for cancer and other angiogenic diseases. Nat. Rev. Drug Discov. *10*, 417–427.

Chan, D.A., Kawahara, T.L., Sutphin, P.D., Chang, H.Y., Chi, J.T., and Giaccia, A.J. (2009). Tumor vasculature is regulated by PHD2-mediated angiogenesis and bone marrow-derived cell recruitment. Cancer Cell *15*, 527–538.

D'Adamo, D.R., Anderson, S.E., Albritton, K., Yamada, J., Riedel, E., Scheu, K., Schwartz, G.K., Chen, H., and Maki, R.G. (2005). Phase II study of doxorubicin and bevacizumab for patients with metastatic soft-tissue sarcomas. J. Clin. Oncol. *23*, 7135–7142.

Date, T., Mochizuki, S., Belanger, A.J., Yamakawa, M., Luo, Z., Vincent, K.A., Cheng, S.H., Gregory, R.J., and Jiang, C. (2005). Expression of constitutively stable hybrid hypoxia-inducible factor-1alpha protects cultured rat cardiomyocytes against simulated ischemia-reperfusion injury. Am. J. Physiol. Cell Physiol. *288*, C314–C320.

Dhar, S., Kolishetti, N., Lippard, S.J., and Farokhzad, O.C. (2011). Targeted delivery of a cisplatin prodrug for safer and more effective prostate cancer therapy in vivo. Proc. Natl. Acad. Sci. USA *108*, 1850–1855.

Eckle, T., Köhler, D., Lehmann, R., El Kasmi, K., and Eltzschig, H.K. (2008). Hypoxia-inducible factor-1 is central to cardioprotection: a new paradigm for ischemic preconditioning. Circulation *118*, 166–175.

Epstein, A.C., Gleadle, J.M., McNeill, L.A., Hewitson, K.S., O'Rourke, J., Mole, D.R., Mukherji, M., Metzen, E., Wilson, M.I., Dhanda, A., et al. (2001). C. elegans EGL-9 and mammalian homologs define a family of dioxygenases that regulate HIF by prolyl hydroxylation. Cell *107*, 43–54.

Fischer, C., Jonckx, B., Mazzone, M., Zacchigna, S., Loges, S., Pattarini, L., Chorianopoulos, E., Liesenborghs, L., Koch, M., De Mol, M., et al. (2007). Anti-PlGF inhibits growth of VEGF(R)-inhibitor-resistant tumors without affecting healthy vessels. Cell *131*, 463–475.

Fraisl, P., Aragonés, J., and Carmeliet, P. (2009). Inhibition of oxygen sensors as a therapeutic strategy for ischaemic and inflammatory disease. Nat. Rev. Drug Discov. *8*, 139–152.

Gerald, D., Berra, E., Frapart, Y.M., Chan, D.A., Giaccia, A.J., Mansuy, D., Pouyssegur, J., Yaniv, M., and Mechta-Grigoriou, F. (2004). JunD reduces tumor angiogenesis by protecting cells from oxidative stress. Cell *118*, 781–794.

Goel, S., Duda, D.G., Xu, L., Munn, L.L., Boucher, Y., Fukumura, D., and Jain, R.K. (2011). Normalization of the vasculature for treatment of cancer and other diseases. Physiol. Rev. *91*, 1071–1121.

Heldin, C.H., Rubin, K., Pietras, K., and Ostman, A. (2004). High interstitial fluid pressure - an obstacle in cancer therapy. Nat. Rev. Cancer *4*, 806–813.

Hofmann, M., Guschel, M., Bernd, A., Bereiter-Hahn, J., Kaufmann, R., Tandi, C., Wiig, H., and Kippenberger, S. (2006). Lowering of tumor interstitial fluid pressure reduces tumor cell proliferation in a xenograft tumor model. Neoplasia *8*, 89–95.

Huang, M., Chan, D.A., Jia, F., Xie, X., Li, Z., Hoyt, G., Robbins, R.C., Chen, X., Giaccia, A.J., and Wu, J.C. (2008). Short hairpin RNA interference therapy for ischemic heart disease. Circulation *118* (14, Suppl), S226–S233.

Hyvärinen, J., Hassinen, I.E., Sormunen, R., Mäki, J.M., Kivirikko, K.I., Koivunen, P., and Myllyharju, J. (2010). Hearts of hypoxia-inducible factor prolyl 4-hydroxylase-2 hypomorphic mice show protection against acute ischemia-reperfusion injury. J. Biol. Chem. *285*, 13646–13657.

Jain, K.K. (2010). Advances in the field of nanooncology. BMC Med. *8*, 83.

Kamphues, C., Wittschieber, D., Klauschen, F., Kasajima, A., Dietel, M., Schmidt, S.C., Glanemann, M., Bahra, M., Neuhaus, P., Weichert, W., and

Stenzinger, A. (2012). Prolyl hydroxylase domain 2 protein is a strong prognostic marker in human gastric cancer. Pathobiology *79*, 11–17.

Kerbel, R.S., and Kamen, B.A. (2004). The anti-angiogenic basis of metronomic chemotherapy. Nat. Rev. Cancer *4*, 423–436.

Kung, A.L., Zabludoff, S.D., France, D.S., Freedman, S.J., Tanner, E.A., Vieira, A., Cornell-Kennon, S., Lee, J., Wang, B., Wang, J., et al. (2004). Small molecule blockade of transcriptional coactivation of the hypoxia-inducible factor pathway. Cancer Cell *6*, 33–43.

Lee, K.A., Lynd, J.D., O'Reilly, S., Kiupel, M., McCormick, J.J., and LaPres, J.J. (2008). The biphasic role of the hypoxia-inducible factor prolyl-4-hydroxylase, PHD2, in modulating tumor-forming potential. Mol. Cancer Res. *6*, 829–842.

Lee, P.J., Jiang, B.H., Chin, B.Y., Iyer, N.V., Alam, J., Semenza, G.L., and Choi, A.M. (1997). Hypoxia-inducible factor-1 mediates transcriptional activation of the heme oxygenase-1 gene in response to hypoxia. J. Biol. Chem. *272*, 5375–5381.

Loges, S., Mazzone, M., Hohensinner, P., and Carmeliet, P. (2009). Silencing or fueling metastasis with VEGF inhibitors: antiangiogenesis revisited. Cancer Cell *15*, 167–170.

Martin, F., Linden, T., Katschinski, D.M., Oehme, F., Flamme, I., Mukhopadhyay, C.K., Eckhardt, K., Tröger, J., Barth, S., Camenisch, G., and Wenger, R.H. (2005). Copper-dependent activation of hypoxia-inducible factor (HIF)-1: implications for ceruloplasmin regulation. Blood *105*, 4613–4619.

Mazzone, M., Dettori, D., Leite de Oliveira, R., Loges, S., Schmidt, T., Jonckx, B., Tian, Y.M., Lanahan, A.A., Pollard, P., Ruiz de Almodovar, C., et al. (2009). Heterozygous deficiency of PHD2 restores tumor oxygenation and inhibits metastasis via endothelial normalization. Cell *136*, 839–851.

Minamishima, Y.A., Moslehi, J., Bardeesy, N., Cullen, D., Bronson, R.T., and Kaelin, W.G., Jr. (2008). Somatic inactivation of the PHD2 prolyl hydroxylase causes polycythemia and congestive heart failure. Blood *111*, 3236–3244.

Minamishima, Y.A., Moslehi, J., Padera, R.F., Bronson, R.T., Liao, R., and Kaelin, W.G., Jr. (2009). A feedback loop involving the Phd3 prolyl hydroxylase tunes the mammalian hypoxic response in vivo. Mol. Cell. Biol. *29*, 5729–5741.

Minotti, G., Menna, P., Salvatorelli, E., Cairo, G., and Gianni, L. (2004). Anthracyclines: molecular advances and pharmacologic developments in antitumor activity and cardiotoxicity. Pharmacol. Rev. *56*, 185–229.

Mukhopadhyay, C.K., Mazumder, B., and Fox, P.L. (2000). Role of hypoxia-inducible factor-1 in transcriptional activation of ceruloplasmin by iron deficiency. J. Biol. Chem. *275*, 21048–21054.

Nakasone, E.S., Askautrud, H.A., Kees, T., Park, J.H., Plaks, V., Ewald, A.J., Fein, M., Rasch, M.G., Tan, Y.X., Qiu, J., et al. (2012). Imaging tumor-stroma interactions during chemotherapy reveals contributions of the microenvironment to resistance. Cancer Cell *21*, 488–503.

Pabla, N., and Dong, Z. (2008). Cisplatin nephrotoxicity: mechanisms and renoprotective strategies. Kidney Int. *73*, 994–1007.

Paterna, J.C., Moccetti, T., Mura, A., Feldon, J., and Büeler, H. (2000). Influence of promoter and WHV post-transcriptional regulatory element on AAV-mediated transgene expression in the rat brain. Gene Ther. *7*, 1304–1311.

Peurala, E., Koivunen, P., Bloigu, R., Haapasaari, K.M., and Jukkola-Vuorinen, A. (2012). Expressions of individual PHDs associate with good prognostic factors and increased proliferation in breast cancer patients. Breast Cancer Res. Treat. *133*, 179–188.

Provenzano, P.P., Cuevas, C., Chang, A.E., Goel, V.K., Von Hoff, D.D., and Hingorani, S.R. (2012). Enzymatic targeting of the stroma ablates physical barriers to treatment of pancreatic ductal adenocarcinoma. Cancer Cell *21*, 418–429.

Rolny, C., Mazzone, M., Tugues, S., Laoui, D., Johansson, I., Coulon, C., Squadrito, M.L., Segura, I., Li, X., Knevels, E., et al. (2011). HRG inhibits tumor growth and metastasis by inducing macrophage polarization and vessel normalization through downregulation of PlGF. Cancer Cell *19*, 31–44.

Schneider, M., Van Geyte, K., Fraisl, P., Kiss, J., Aragonés, J., Mazzone, M., Mairbäurl, H., De Bock, K., Jeoung, N.H., Mollenhauer, M., et al. (2010). Loss or silencing of the PHD1 prolyl hydroxylase protects livers of mice against ischemia/reperfusion injury. Gastroenterology *138*, 1143–1154.

Scortegagna, M., Ding, K., Oktay, Y., Gaur, A., Thurmond, F., Yan, L.J., Marck, B.T., Matsumoto, A.M., Shelton, J.M., Richardson, J.A., et al. (2003). Multiple organ pathology, metabolic abnormalities and impaired homeostasis of reactive oxygen species in Epas1-/- mice. Nat. Genet. *35*, 331–340.

Semenza, G.L. (2003). Targeting HIF-1 for cancer therapy. Nat. Rev. Cancer *3*, 721–732.

Shokolenko, I., Venediktova, N., Bochkareva, A., Wilson, G.L., and Alexeyev, M.F. (2009). Oxidative stress induces degradation of mitochondrial DNA. Nucleic Acids Res. *37*, 2539–2548.

Stockmann, C., Doedens, A., Weidemann, A., Zhang, N., Takeda, N., Greenberg, J.I., Cheresh, D.A., and Johnson, R.S. (2008). Deletion of vascular endothelial growth factor in myeloid cells accelerates tumorigenesis. Nature *456*, 814–818.

Su, Y., Loos, M., Giese, N., Metzen, E., Büchler, M.W., Friess, H., Kornberg, A., and Büchler, P. (2012). Prolyl hydroxylase-2 (PHD2) exerts tumor-suppressive activity in pancreatic cancer. Cancer *118*, 960–972.

Takeda, K., Cowan, A., and Fong, G.H. (2007). Essential role for prolyl hydroxylase domain protein 2 in oxygen homeostasis of the adult vascular system. Circulation *116*, 774–781.

Takeda, Y., Costa, S., Delamarre, E., Roncal, C., Leite de Oliveira, R., Squadrito, M.L., Finisguerra, V., Deschoemaeker, S., Bruyère, F., Wenes, M., et al. (2011). Macrophage skewing by Phd2 haplodeficiency prevents ischaemia by inducing arteriogenesis. Nature *479*, 122–126.

Unnikrishnan, A., Raffoul, J.J., Patel, H.V., Prychitko, T.M., Anyangwe, N., Meira, L.B., Friedberg, E.C., Cabelof, D.C., and Heydari, A.R. (2009). Oxidative stress alters base excision repair pathway and increases apoptotic response in apurinic/apyrimidinic endonuclease 1/redox factor-1 haploinsufficient mice. Free Radic. Biol. Med. *46*, 1488–1499.

Van der Veldt, A.A., Lubberink, M., Bahce, I., Walraven, M., de Boer, M.P., Greuter, H.N., Hendrikse, N.H., Eriksson, J., Windhorst, A.D., Postmus, P.E., et al. (2012). Rapid decrease in delivery of chemotherapy to tumors after anti-VEGF therapy: implications for scheduling of anti-angiogenic drugs. Cancer Cell *21*, 82–91.

Vengellur, A., Woods, B.G., Ryan, H.E., Johnson, R.S., and LaPres, J.J. (2003). Gene expression profiling of the hypoxia signaling pathway in hypoxia-inducible factor 1alpha null mouse embryonic fibroblasts. Gene Expr. *11*, 181–197.

Vengellur, A., Grier, E., and Lapres, J.J. (2011). The Loss of HIF1α Leads to Increased Susceptibility to Cadmium-Chloride-Induced Toxicity in Mouse Embryonic Fibroblasts. J. Toxicol. *2011*, 391074.

Winkler, F., Kozin, S.V., Tong, R.T., Chae, S.S., Booth, M.F., Garkavtsev, I., Xu, L., Hicklin, D.J., Fukumura, D., di Tomaso, E., et al. (2004). Kinetics of vascular normalization by VEGFR2 blockade governs brain tumor response to radiation: role of oxygenation, angiopoietin-1, and matrix metalloproteinases. Cancer Cell *6*, 553–563.